

EXPERIMENTS AND SIMULATIONS OF LARGE SCALE HYDROGEN-NITROGEN-AIR GAS EXPLOSIONS FOR NUCLEAR AND HYDROGEN SAFETY APPLICATIONS

Lucas M.¹, Salaün N.², Atanga G.³, Wilkins B. ⁴, Martin-Barbaz S.⁵

**¹Software, Gexcon AS, Fantoftvegen 38, Bergen, 5072, Norway,
Melodia.Lucas.Perez@gexcon.com**

**²Consulting, Gexcon AS, Fantoftvegen 38, Bergen, 5072, Norway,
Nicolas.Salaun@gexcon.com**

**³Software, Gexcon AS, Fantoftvegen 38, Bergen, 5072, Norway,
Gordon.Atanga@gexcon.com**

**⁴Fire & Explosion testing, Gexcon AS, Fantoftvegen 38, Bergen, 5072, Norway,
Brian.Wilkins@gexcon.com**

**⁵ Direction Technique, EDF, 19 rue Bourdeix, Lyon, 69007, France,
sebastien.martin-barbaz@edf.fr**

ABSTRACT

Hydrogen safety is a general concern because of the high reactivity compared to hydrocarbon-based fuels. The strength of knowledge in risk assessments related to the physical phenomena and the ability of models to predict the consequence of accidental releases is a key aspect for the safe implementation of new technologies. Nuclear safety considers the possibility of accidental leakages of hydrogen gas and subsequent explosion events in risk analysis. In many configurations, the considered gaseous streams involve a large fraction of nitrogen gas mixed with hydrogen. This work presents the results of a large scale explosion experimental campaign for hydrogen-nitrogen-air mixtures. The experiments were performed in a 50 m³ vessel at Gexcon's test site in Bergen, Norway. The nitrogen fraction, the equivalence ratio and the congestion level were investigated. The experiments are simulated in the FLACS-CFD software to inform about the current level of conservatism of the predictions for engineering application purposes. The study shows the reduced overpressure with nitrogen added to hydrogen mixtures and supports the use of FLACS-CFD-based risk analysis for hydrogen-nitrogen scenarios.

1.0 INTRODUCTION

There is currently a major drive to promote hydrogen as a substitute to fossil fuel sources, as it can be a key enabler for the decarbonisation of the industry, the transport or the power generation sectors. Hydrogen has been used in the industry for years and has served as a powerful rocket fuel for decades. However, the high reactivity [1] compared to hydrocarbon-based fuels arises safety related challenges for adopting a wider use of hydrogen-based technologies. In a nuclear power plant, hydrogen is present as a waste resulting from electrolysis in the primary nuclear water-based cooling system, as a heat carrier used to cool down the alternator in the non-nuclear part of the power plant and as a corrosion inhibitor. Hydrogen is therefore included as part of the risk assessment of nuclear power plants. Part of a risk assessment entails the consequence analysis of the identified hazards. CFD (Computational Fluid Dynamic) tools are useful for consequence analysis of accidental hydrogen releases and the possible outcomes, such as fire or explosions in complex

geometries. Salaün et al. [2] and Chillè et al. [3,4] discussed the various assumptions needed for simplified structural assessments that increase the man-hour effort and affect the results. They show reduced user-dependent methodologies based on one-way coupling CFD and FE (Finite Elements) calculations to perform consequence analysis, design verification and structural response studies in nuclear power plants for accidental hydrogen releases. Even though process gas streams in nuclear power plants contain a large fraction of gaseous nitrogen (often in the range of 30-50 vol.% and sometimes up to 70 vol.%), pure hydrogen was assumed to ensure a certain degree of conservatism in the safety assessment. In 2001, Gexcon performed a small-scale experimental program involving hydrogen and 75 vol.% hydrogen-25 vol.% nitrogen blends explosion tests in a squared channel (0.3 m x 0.3 m x 1.44 m) and in a congested corner-like configuration (0.37 m x 0.37 m x 0.37) [5]. Both experiment observations and simulation [6] predictions show a decrease in maximum overpressure with nitrogen addition. This paper shows the explosion overpressure results of a larger scale (2.5 m diameter and 10.35 m long tube) hydrogen-nitrogen experimental campaign and comparison to predictions by the CFD based model system FLACS. The experimental program, conducted in 2019 at the Gexcon's test site in Norway, studies the influence of various nitrogen contents on the explosion severity, for various equivalence ratios (ER) and different congestion levels. The tests are simulated with FLACS to qualify its robust and conservative use for engineering purposes and to serve as a basis for model improvements in the areas where overprediction is considered important for safety engineering purposes.

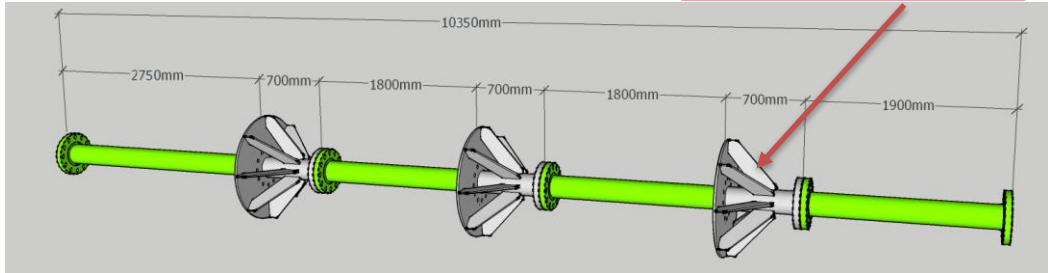
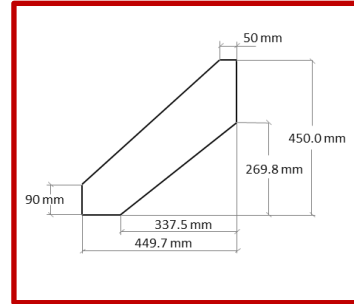
2.0 EXPERIMENTAL SET UP

Figure 1a shows the vessel where the experiments were performed. The 50 m³ cylindrical vessel, with a length of 10.35 m and an inner diameter of 2.5 m, is open at one end. The vessel was anchored to the ground and restrained by concrete blocks and two recoil-beams behind the closed end.

Different obstructions were used in the vessel providing different levels of congestion. The pipes were 8'' diameter with mounting flanges of 0.46 m and 0.05 m thickness. Figure 1b shows the length of the pipes with its flanges and illustrates the 3x20% geometry configuration. The 3x20% geometry consisted of three plates blocking 20% of the vessel's cross section. In the 1x20% geometry, one plate with 20% blockage was mounted between the 2.75 m and the 1.8 m pipes, the obstructions in Figure 1b after 5.25 m were not used in this geometry type. In the 1x30 % geometry, a 30% blocking plate was placed at 7.75 m from the back end, all the mounting pipes were used in this scenario. In the Empty geometry, only the 2.75 m long pipe with its two flanges was placed at the back of the vessel. Table 1 to Table 4 in Appendix A show the experimental configuration.



(a) Cylindrical vessel



(b) 3x20% geometry obstacles placed in the vessel.

Figure 1. Experimental test site and illustration with measurements of the obstructions used in the 3x20% geometry configuration.

2.1 Gas filling system

Hydrogen of grade 3.7 (purity 99.97%) and nitrogen of grade 2.5 (purity 99.5%) were used to prepare the fuel gas in the tests. The gas mixtures were prepared using a re-circulation system consisting of a centrifugal fan and two sets of 8" butterfly valves enabling the gas mixing system to be isolated from the explosion chamber prior to ignition. The fuel gas was added to the re-circulated flow, the amount of gas added was reduced steadily as the desired gas concentration was approached. The ratio between hydrogen and nitrogen was regulated using flow controllers from Brooks Instrument of the type SLA5853. The output from the flow regulators were mixed inside a mixer before being added to the re-circulation system. The gas composition in the mixer was monitored using a binary gas analyser of the type BGA244 from Stanford Research Systems Inc. The oxygen concentration inside the vessel was monitored at three different points using a paramagnetic oxygen analyser of the type Servomex Xendos 2223.

2.2 Instrumentation

An oscillating electrical spark was used to initiate the explosions. The ignition source was located close to the central axis at approximately one meter from the closed end of the vessel. The overpressure was measured using five piezo-electric pressure transducers with a frequency response of 70 kHz from Kistler (type 701A) connected to Kistler charge amplifiers (type 5073A). The measurements were recorded with a sampling rate of 100kHz. The pressure transducers were mounted along the central longitudinal axis at the top of the vessel, P1 at 2 m, P2 at 4 m, P3 at 6 m and P4 at 8 m from the close end.

3.0 FLACS-Hydrogen AND MODEL SETUP

FLACS-Hydrogen is a sub-module of the CFD based model system FLACS-CFD [7] for hydrogen safety applications that was first developed in connection with the Network of Excellence (NoE) HySafe, funded by the European Commission [8]. Several R&D projects have contributed to the development of the tool and to extend the validation database for hydrogen applications [8,9].

FLACS uses the porosity/distributed resistance (PDR) approach for representing complex geometries smaller than the control volume. The Reynolds-averaged Navier-Stokes (RANS) equations are solved on an strutted Cartesian grid using a finite volume method. The code applies the standard $k-\varepsilon$ turbulence model [10] modified to account for sub-grid contributions.

The conservation equation for the fuel mass fraction, Y_F , is expressed as

$$\frac{\partial}{\partial t} (\beta_v \rho Y_F) + \frac{\partial}{\partial x_j} (\beta_j \rho u_j Y_F) = \frac{\partial}{\partial x_j} \left(\beta_j \rho D \frac{\partial Y_F}{\partial x_j} \right) + R_F, \quad (3)$$

where the diffusion coefficient, D , and the chemical reaction source term, R_F , are given by

$$D = C_{\beta D} s \Delta \text{ and } R_F = C_{\beta R F} \frac{S}{\Delta} \rho \min \left(1 - \frac{Y_F}{Y_{F0}}, 9 \frac{Y_F}{Y_{F0}} \right). \quad (4)$$

Here, $C_{\beta D}$ and $C_{\beta R F}$ are model constants, s is the burning velocity, Δ is the control volume length in the direction of flame propagation and Y_{F0} is the initial fuel mass fraction.

The laminar burning velocity at atmospheric pressure, s_{L0} , is tabulated for different ER. FLACS-CFD applies a correction to the hydrogen laminar burning velocity based on the Lewis number, $s_{L,Le}$. To model the regime of cellular flame propagation the quasi-laminar burning velocity concept is used. The quasi-laminar burning velocity, s_{QL} , is modelled as [11]

$$s_{QL} = s_{L,Le} (1 + C_{QL} r_F^a), \quad (5)$$

where C_{QL} is a mixture-dependent model constant, r_F is the flame radius and a is a model constant. The turbulent burning velocity, s_T , is expressed in terms of the effective root-mean-square turbulence velocity, u' , and the Karlovitz stretch factor, K , following Bradley et al. [12]

$$\frac{s_T}{u'} = \alpha K^{-\beta}, \quad K = 0.25 \left(\frac{u'}{s_{L,Le}} \right)^2 \left(\frac{u' l_C}{\nu} \right)^{-0.5}, \quad (7)$$

with constant α and β empirical parameters. Here ν is the kinematic viscosity and l_C is the combustion length scale. l_C is proportional to the distance from the point of ignition to the flame front bounded by a parameter that is proportional to the distance between the enclosing walls.

The low intensity turbulent burning velocity correlation is [11]

$$s_T = 0.96 u'^{0.912} s_L^{0.284} \frac{l_C^{0.196}}{\nu} + s_L. \quad (10)$$

Turbulence and flame folding sub-grid models enhance the burning velocity due to contribution from sub-grid objects. Thus, convergence of the model predictions are not necessarily expected for gradual refinement of the computational grid. Users of FLACS must therefore follow the grid guidelines provided in the User's Manual [7] which are derived from validation of the software against an extensive experimental database. Figure 2 shows the geometry with area and volume porosities for the 15 cm grid used in the FLACS *v10.9* simulations for the 3x20% geometry configuration.

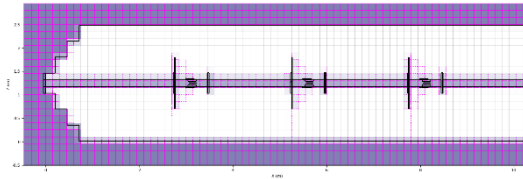


Figure 2. Grid resolution with area and volume porosities for the 3x20% geometry configuration.

4.0 RESULTS

The experimental pressure-time series were filtered using a second order Savitzky-Golay filter with a frame size of 1.5 ms. The offset in the pressure was corrected through alignment to zero at the ignition time. For tests without obstacles inserted (Empty) two distinct pressure peaks were measured. The second peak was attributed to an external explosion. For tests with obstacles, more than two peaks were often observed which are related to the interaction with the obstacles. However, since there was no visual access inside the tube, it is difficult to analyse the cause of each peak in more detail. Thus, the overall maximum peak is used for comparison of the measured to the simulated values.

During the experimental campaign several tests were repeated to give an indication of the reproducibility of the system. All repeated tests were performed in the 3x20% geometry. Figure 3 and Figure 4 show the observed and predicted pressure-time curves at P1 and P4 for Test07/Test11 and Test17/Test19. A very good reproducibility was observed. The maximum difference in measured overpressure was 14% for Test07/Test11 at P4 and 7% for Test17/Test19 at P1.

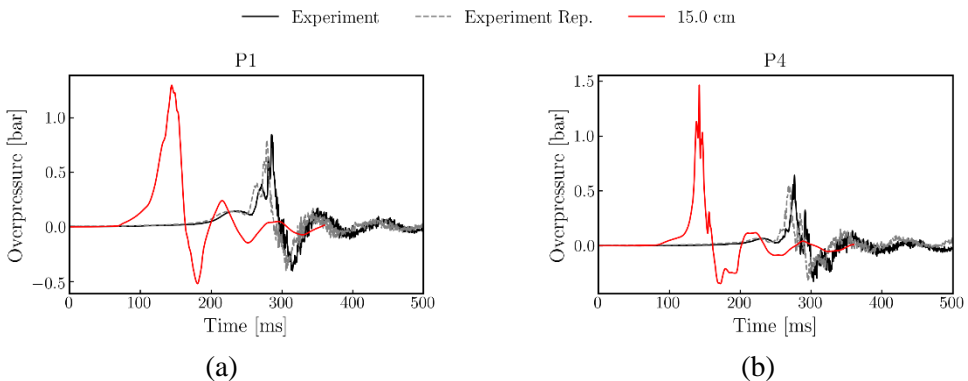


Figure 3. Experiment (Test07) vs repetition (Test11) at pressure transducer P1 (a) and at pressure transducer P4 (b).

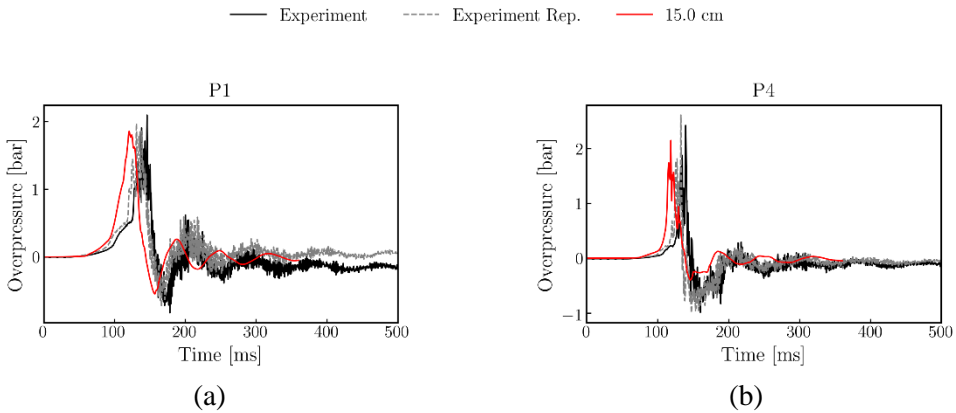


Figure 4. Experiment (Test17) vs repetition (Test19) at pressure transducer P1 (a) and at pressure transducer P4 (b).

Figure 5 shows the pressure time curves at P1 and P5 for Test09/Test13 with 75 vol.% hydrogen. The maximum overpressure for Test13 at P1 was about 1.3 times the measured overpressure for Test09 at P1. There is a sharp pressure peak of 11.7 bar at P5 when the flame exits the vessel. The flame speed from high-speed video analysis was estimated to be between 1500 to 2000 m/s, suggesting that a deflagration-to-detonation transition (DDT) occurred inside the vessel. This was also observed for Test13, Test10 and Test27. For Test13, the DDT happened earlier in the vessel compared to Test09. In this type of scenario, small instabilities or deviations in the initial conditions can trigger detonation earlier and therefore enhance the differences in the results.

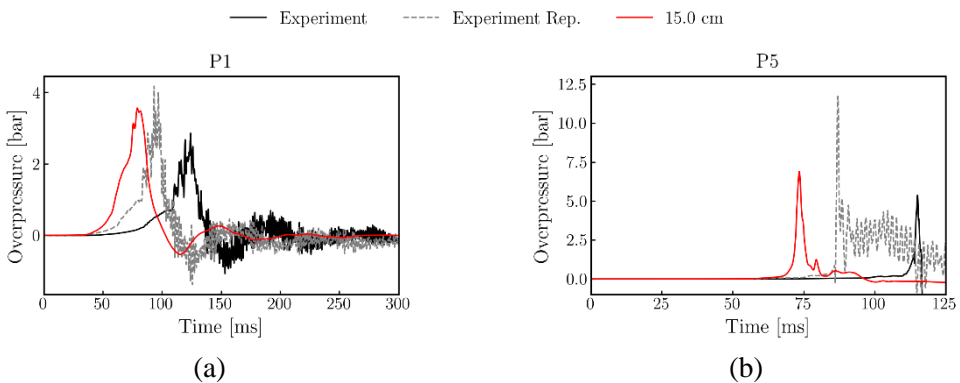


Figure 5. Experiment (Test09) vs repetition (Test13) at pressure transducer P1 (a) and at pressure transducer P5 (b).

FLACS *v10.9* cannot model the transition from deflagration to detonation (DDT) directly, the simulation is considered as a deflagration even when the flame front reaches the pressure front. However, it can give an indication of the likelihood of DDT occurrence. The DPDX (normalised spatial pressure gradient across the flame front) is used to determine whether there is a possibility of detonation, for hydrogen explosions $DPDX > 1$ indicates that a DDT

is possible and $DPDX > 5$ that DDT is likely to occur [6]. For Test09, Test10, and Test13 simulations predict $DPDX$ values of above 1 close to the second blocking plate and up to 6 close to the third blocking plate. For Test27 $DPDX$ values are about 1 at the end of the pipe flange indicating that a DDT may occur inside the vessel. The highest maximum measured overpressure was 12.38 bar and occurred for Test10, with the most congested geometry (3x20%) and with 100% H_2 , at sensor P5 located right before the end of the vessel. The predicted maximum overpressure occurred also for Test10 at P5. However, the peak is underpredicted since detonation is not considered. The lowest maximum measured overpressure was 10.65 mbar and occurred for Test 32, with the largest amount of N_2 used, 80% N_2 , and with the 1x20% geometry. The lowest predicted maximum overpressure occurred also for Test32 and was 9.85 mbar. The tests where DDT was identified inside the vessel are not included in the further discussions.

Figure 6 shows the maximum overpressure inside the vessel against the ER for ignition of the hydrogen-nitrogen clouds for different congestion levels. The experimental results are represented by black circles and the simulation results with the 0.15 m grid by red squares. The grey symbols correspond to simulations with grid sizes 0.20 m and 0.25 m which are not recommended by the latest FLACS user manual [13]. The measured maximum overpressure in the experiments is highest for $ER=1$ and decreases for lean and rich mixtures. Model predictions are within a factor of 2 of the values observed in the experiments for stoichiometric mixtures at high blockage ratio (3x20% geometry tests). The simulated maximum overpressure decreases from stoichiometric to rich mixtures in line with measurements but deviate in trend towards lean mixtures for all congestion levels. FLACS applies a Lewis number dependency correction to the laminar burning velocity [8]. The correction for hydrogen mixtures to account for thermal-diffusive effects with varying Lewis or Markstein numbers enhances the laminar burning velocity for $ER < 1.0$ and reduces the laminar burning velocity for $ER > 1.0$. The implemented correction is used for all flow regimes and most likely contributes to the over-prediction of the reactivity for lean and rich hydrogen-air mixtures [14]. The overpressure in Figure 6a for $ER=1$, correspond to Test17 plotted in Figure 4. Even though the simulated overpressure is lower than the observed overpressure, the duration of the peak is similar, and the positive pressure impulse is higher than the observed in experiments. For structural response studies, both maximum overpressure and duration are typically considered when not the whole signal is considered [3]. Therefore, the predictions for this test for structural response analysis are still conservative.

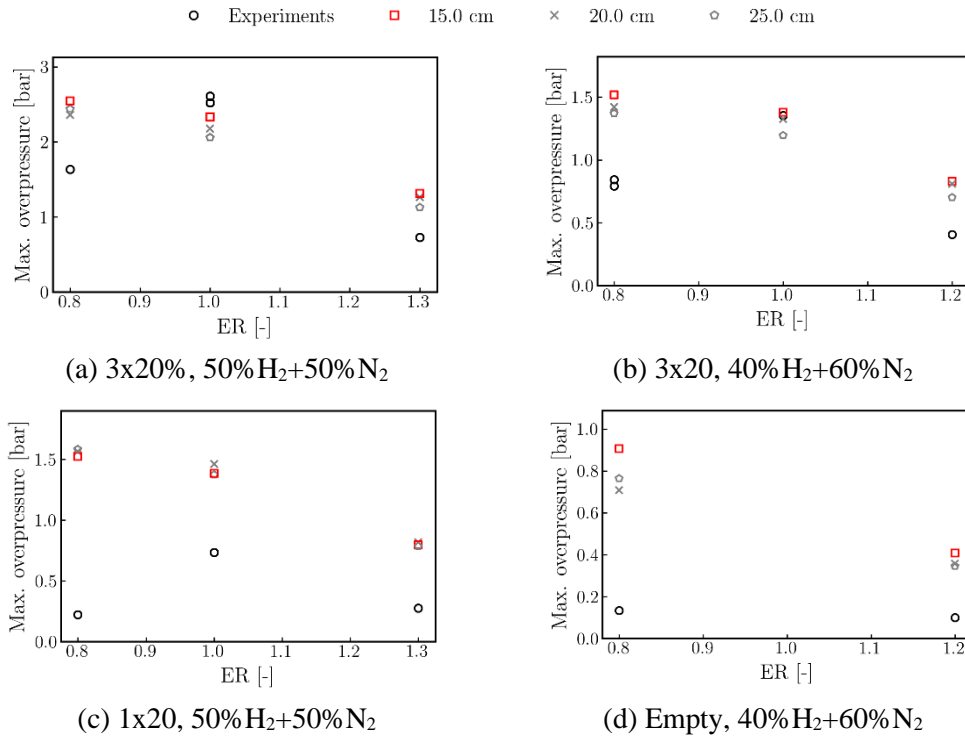


Figure 6. Maximum overpressure against ER.

Figure 7 shows the maximum overpressure inside the vessel for ignition of the hydrogen-nitrogen clouds with an equivalence ratio of 0.8 for different congestion levels. The horizontal axis shows the volumetric nitrogen fraction in the fuel. Both the measured and the predicted maximum overpressure decreases with increasing nitrogen concentration in the premixed cloud. The decrement is more pronounced for the most congested (Figure 7d) than for the low congested (Figure 7b and 7c) and the uncongested geometries (Figure 7a). For Test12 with 40 vol.% nitrogen the peak overpressure was 2.54 bar for Test14 with 50 vol.% nitrogen the peak overpressure was reduced to 1.63 bar and for Test07/Test09 with 60 vol.% the peak overpressure was reduced to 0.84/0.79 bar. Similar trends are observed in the tests with ER=1.0 (Figure 8). The decrease in maximum overpressure with increasing nitrogen content is more pronounced for the 3x20% geometry than for the 1x20% geometry.

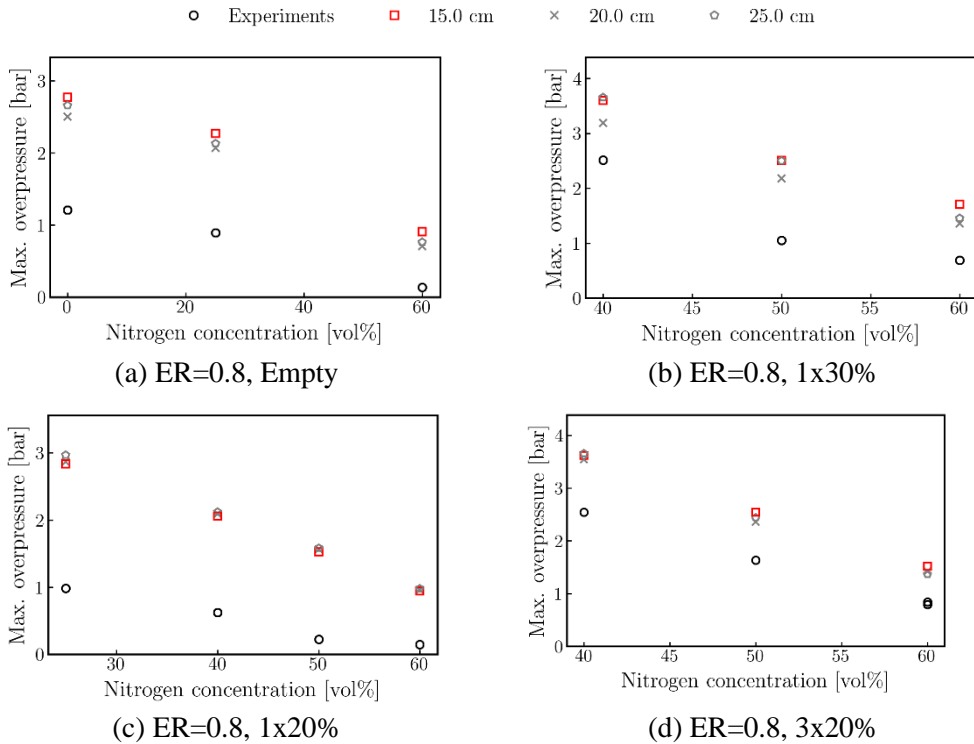


Figure 7. Maximum overpressure against nitrogen concentration for ER=0.8.

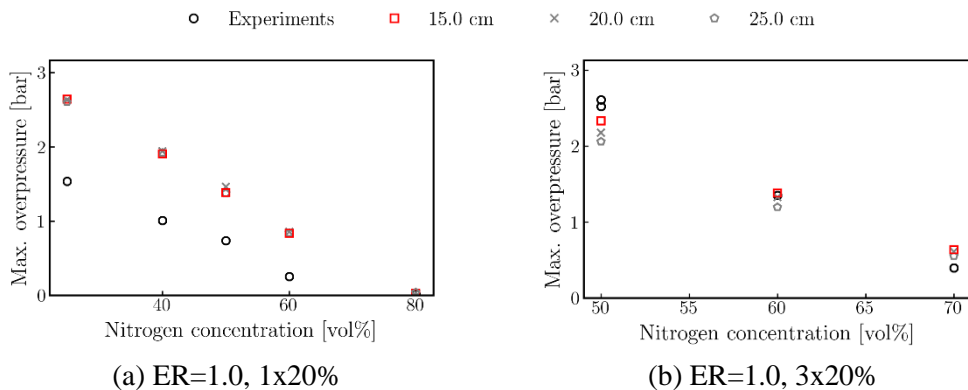


Figure 8. Maximum overpressure against nitrogen concentration for ER = 1 for the 1x20 (a) and the 3x20 (b) geometries.

The peak overpressure increased considerably when adding blocking plates in the vessel. The maximum overpressure for Test28 (ER=0.8, 40 vol.% hydrogen) with one plate blocking 20% of the area is about 6 times lower than for Test07/Test11 (ER=0.8, 40 vol.% hydrogen) with three plates blocking 20% of the area. For Test29 (ER=1, 40 vol.% hydrogen) with only one plate, the maximum overpressure is 5 times lower than the maximum overpressure observed for Test15 (ER=1, 40 vol.% hydrogen) with three plates.

In summary, the maximum overpressure increases with increasing congestion level in the vessel for both experiments and simulations. The peak overpressure decreases with the amount of nitrogen in the mixture, demonstrating the inerting capabilities of nitrogen in hydrogen deflagrations. This trend is also captured by FLACS. The maximum observed overpressure decreases for rich and lean mixtures relative to the stoichiometric value. However, contrary to the experimental observations, the maximum overpressure increases from stoichiometric to lean mixtures, resulting in overpredictions for lean hydrogen-air and hydrogen-nitrogen-air mixtures of more than a factor of 2 of the values observed in the experiments. Based on the work by the Model Evaluation Group for Gas Explosions (MEGGE) [15] and the validation framework proposed by Skjold et al. [16], a model performance is acceptable if at least 50% of the predictions are within a factor of 2 of the measurements. Figure 9 shows the simulation predictions vs the experimental maximum overpressure in a scatter plot where 54% of the values are within a factor of 2 of the experimental measurements. The largest overpredictions occur for scenarios with overpressures lower than 0.2 bar.

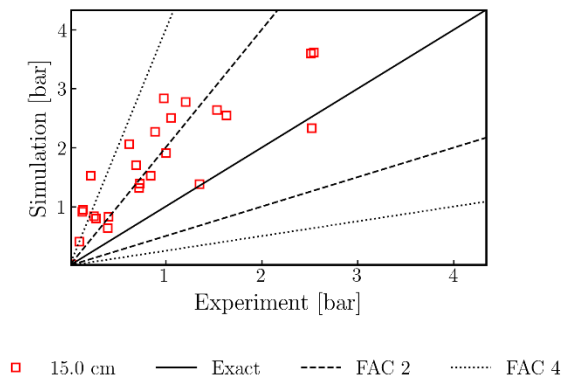


Figure 9. Scatter plot of maximum overpressure inside the vessel.

5.0 CONCLUSION

Experiments were performed in a large and open at one end vessel to investigate hydrogen-nitrogen-air explosions. The effect of varying the blockage ratio, the nitrogen concentration and the ER of the mixture were investigated as representative variables for industry-based applications. A validation study was performed with FLACS *v10.9*. While documenting the level of accuracy of the predictions, the aim of this work was to qualify the safe and conservative use of the software on industrial engineering applications involving a wider range of hydrogen mixtures with significant amount of nitrogen. The outcome led to documenting and/or reducing the level of inappropriate over conservatism in the safety analysis for nuclear powerplants.

The highest maximum measured overpressure occurred for a scenario with the most congested geometry (3x20%) and with 100% H₂ (Test10). The lowest maximum measured overpressure occurred for a test with the largest amount of N₂ considered, 80% N₂, and with the 1x20% geometry (Test32). Deflagration-to-detonation transition was observed at four tests, Test09, Test10, Test13 and Test27, all of them performed in the congested vessel with

hydrogen concentration larger than 75%. FLACS-CFD predicted the possibility of deflagration-to-detonation transition for scenarios where detonation was identified during the experimental campaign.

The predicted maximum overpressure is overconservative in most of the scenarios. For the scenarios where the maximum overpressure is underpredicted, the pressure impulse is conservative. A certain degree of overprediction is acceptable for safety studies where highly conservative predictions can be acceptable when the purpose is to perform a robust safety demonstration. However, for design and/or assessment studies where response analysis and performance standards shall be verified, highly conservative estimates can result in design challenges or unnecessary larger costs. In the current work, the largest overpredictions are observed for the experimental cases with peak overpressures in the lowest range, leading to limited concerns for the civil work and hence the engineering aspects. For evaluating the validity of the model systems for structural response analysis additional parameters should be considered such as the duration of the peak, the pressure impulse and the time of peak occurrence.

ACKNOWLEDGEMENT

The authors gratefully acknowledge the financial support of EDF as co-funding the experimental and validation campaign.

REFERENCES

- [1] HySafe Program, Hydrogen Fundamentals, 2007.
- [2] Salaün, N., Chillè, F., Daudey, N., Structural response based on CFD blast analyses: part I, application to nuclear safety, methodology for design verification of a nuclear power plant against confined hydrogen explosions, CONFAB 2017, London, September 2017.
- [3] Chillè, F., Salaün, N., Daudey, N., Structural response based on CFD blast analyses: part II, application to reinforced concrete structures, CONFAB 2017, London, September 2017.
- [4] Chillè, F., Salaün, N., Daudey, N., Structural response based on CFD blast analyses: part III, application to industrial equipment, CONFAB 2017, London, September 2017.
- [5] Renoult, J., Wilkins, B., Hydrogen explosion safety phase 2 – small scale explosion experiments, GexCon-3-F46201- 2, Confidential.
- [6] Renoult, J., Hansen, O.R., Hydrogen explosion safety phase 3 – FLACS explosion simulations, GexCon-03-F46201 - 4, Confidential.
- [7] Gexcon AS, FLACS v10.9 User's Manual. Bergen, Norway : Gexcon AS, 2019.
- [8] Middha, P., Development, use, and validation of the CFD tool FLACS for hydrogen safety studies, PhD thesis, Department of Physics and Technology, University of Bergen, Norway, 2010.
- [9] M. Lucas, G. Atanga , H. Hisken, L. Mauri, T. Skjold, Simulating vented hydrogen deflagrations: Improved modelling in the CFD tool FLACS-hydrogen, International Journal of Hydrogen Energy 46 (2021) 12464-12473.

- [10] D.B. Launder, B.E. Spalding, The numerical computation of turbulent flows, *Computer Methods in Applied Mechanics and Engineering* 3 (1974) 269 – 289.
- [11] Arntzen B.J., Modelling of turbulence and combustion for simulation of gas explosions in complex geometries, PhD thesis, Department of Energy and Process Engineering, Norwegian University of Science and Technology, Norway, 1998.
- [12] Bradley D., Lawes M., Liu K., Mansour M., Measurements and correlations of turbulent burning velocities over wide ranges of fuels and elevated pressures, *Proceedings of the Combustion Institute*, 34 (2013), 1519 – 1526.
- [13] Gexcon AS, FLACS-CFD 22.1 User's Manual. Bergen, Norway : Gexcon AS, 2022.
- [14] H. Hisken, Investigation of instability and turbulence effects on gas explosions: experiments and modelling, PhD thesis, University of Bergen, Norway, 2018.
- [15] Model Evaluation Group Gas Explosions (MEGGE). (1996). Gas Explosion Model Evaluation Protocole, Version 1, Technical Report.
- [16] Skjold, T., Pedersen, H.H., Bernard, L., Ichard, M., Middha, P., Narasimhamurthy, V.D., Landvik, T., Lea, T & Pesch, L. (2013). A matter of life and death: validating, qualifying and documenting models for simulating flow-related accident scenarios in the process industry, *Chemical Engineering Transactions*, 31: 187-192.

APPENDIX A – EXPERIMENTAL SETUP

Table 1. Experimental setup for the tests performed in the Empty geometry

Test	H ₂ [vol.%]	N ₂ [vol.%]	ER [-]	Geometry	T [°C]
1	100	0	0.8	Empty	16.5
2	75	25	0.8	Empty	17.6
3	40	60	0.8	Empty	18.9
4	40	60	1.2	Empty	14.1
5	75	25	1.2	Empty	15.3
6	100	0	1.2	Empty	15.4

Table 2. Experimental setup for the tests performed in the 1x20% geometry

Test	H ₂ [vol.%]	N ₂ [vol.%]	ER [-]	Geometry	T [°C]
22	50	50	1.0	1x20%	11.3
23	60	40	0.8	1x20%	13.3
24	75	25	0.8	1x20%	11.8
25	60	40	1.0	1x20%	12.9
26	75	25	1.0	1x20%	14.9
27	100	0	0.8	1x20%	9.8
28	40	60	0.8	1x20%	10.6
29	40	60	1.0	1x20%	9.7
30	50	50	1.3	1x20%	9.7
31	50	50	0.8	1x20%	9.8
32	20	80	1.0	1x20%	12.2
33	60	40	1.0	1x20%	12.7

Table 3. Experimental setup for the tests performed in the 3x20% geometry

Test	H ₂ [vol.%]	N ₂ [vol.%]	ER [-]	Geometry	T [°C]
7	40	60	0.8	3x20%	15.4
8	40	60	1.2	3x20%	15.4
9	75	25	0.8	3x20%	14.6
10	100	0	0.8	3x20%	16.2
11	40	60	0.8	3x20%	15.3
12	60	40	0.8	3x20%	16.7
13	75	25	0.8	3x20%	16.8
14	50	50	0.8	3x20%	22.9
15	40	60	1.0	3x20%	15.0
16	30	70	1.0	3x20%	14.6
17	50	50	1.0	3x20%	16.4
18	50	50	1.3	3x20%	16.0
19	50	50	1.0	3x20%	15.2
21	30	70	1.2	3x20%	16.1

Table 4. Experimental setup for the tests performed in the 1x30% geometry

Test	H ₂ [vol.%]	N ₂ [vol.%]	ER [-]	Geometry	T [°C]
36	50	50	0.8	1x30%	17.7
37	50	50	1.3	1x30%	17.7
38	60	40	0.8	1x30%	12.6
39	40	60	0.8	1x30%	12.2
40	40	60	1.2	1x30%	12.1